Long-lived χ_1^0 in Gauge Mediated SUSY Breaking

N. Wattimena[1,2], J. List[2]

1- Institut für Experimentalphysik der Universität Hamburg
Luruper Chaussee 149
D-22761 Hamburg, Germany

2- Deutsches Elektronen Synchrotron DESY
Notkestr. 85
D-22607 Hamburg, Germany

1 Gauge Mediated SUSY Breaking

In the course of detector optimisation, a very challenging process for the electromagnetic calorimeter (ECAL) is the reconstruction of highly energetic, non-pointing photons. This signature could e.g. appear from the decay of long-lived supersymmetric (SUSY) particles. To reconstruct the mass and lifetime of the originating SUSY particle requires both, good photon energy reconstruction, and excellent photon pointing resolution. Thus, it is a good way to test the electromagnetic calorimeter performance.

Supersymmetry is a promising extension to the Standard Model (SM) of particle physics. It could solve many open questions, e.g. the matter-antimatter-asymmetry, by combining bosons and fermions in supermultiplets. On the other hand it introduces many new free parameters, which would have to be measured. Even a minimum extension to the Standard Model requires more than one hundred additional free parameters [1].

As of today no supersymmetric particles have been discovered, thus the SUSY partners must be heavier than their SM partner and SUSY has to be a broken symmetry. In gauge-mediated SUSY breaking (GMSB) scenarios, the breaking occurs at an energy scale $\sqrt{F}$ much smaller than the Planck-scale. Chiral superfields belonging to an intermediate messenger sector at an energy scale M_{mess}, transfer the breaking to the minimal supersymmetric SM sector. Since the gravitino $\tilde{G}$ gets its mass from gravitational interactions only, it is the lightest SUSY particle (LSP) [2]. Assuming R-parity conservation, only five parameters and a sign are needed to determine a GMSB SUSY spectrum. The soft SUSY breaking scale Λ, the number of messenger chiral supermultiplets N_5, the messenger mass scale M_{mess}, the ratio of the Higgs vacuum expectation values $\tan(\beta)$, the scale factor for the gravitino mass c_{grav}, and the sign of the Higgs mass parameter $\mathrm{sgn}(\mu)$ [1]. Depending on their values, the next-to-lightest SUSY particle (NLSP) can either be the lightest right-handed slepton $\tilde{l_{\mathrm{R}}}$, or the lightest neutralino $\tilde{\chi}_1^0$. The NLSP would inevitably decay into the LSP and its SM partner. As a feature of GMSB this can happen after a finite decaytime, corresponding to a distance from microns to kilometres, depending on the mass difference between the NLSP and LSP:

$$c\tau = \frac{1}{k_\gamma} \cdot \left(\frac{100\ \mathrm{GeV}}{m_{\mathrm{NLSP}}}\right)^5 \cdot \left(\frac{\sqrt{F}}{100\ \mathrm{TeV}}\right)^4 \cdot 10^{-2}\ \mathrm{cm}\ , \tag{1}$$

where

$$F = c_{\mathrm{grav}} \cdot \Lambda \cdot M_{\mathrm{mess}}\ . \tag{2}$$

is the SUSY breaking scale.

$$k_\gamma \equiv |N_{11}\cos\theta_W + N_{12}\sin\theta_W| \tag{3}$$

with the Weinberg angle θ_W, and neutralino mixing angles N_{ij}.

In the following, we consider scenarios where the NLSP is a neutralino, decaying into the LSP $\tilde{\chi}_1^0 \rightarrow \tilde{G}\gamma$ several cm from the initial interaction point (IP). For $e^+e^- \rightarrow \tilde{\chi}_1^0\tilde{\chi}_1^0$ events, the topology, which is two highly energetic photons and missing energy, might be mimicked by SM processes that include two photons, eventually missing energy from neutrinos, and nothing else.

2 Event Simulation

2.1 SUSY Spectrum Generation

The SUSY spectrum is calculated with SPheno [3]. The chosen input variables fulfil the requirements given in [4], and are chosen to be:

$$\Lambda = 110\,\mathrm{TeV}\,, \quad \mathrm{M_{mess}} = 240\,\mathrm{TeV} \quad \mathrm{N_5} = 1\,, \quad \tan(\beta) = 3.0\,, \quad \mathrm{sgn}(\mu) = +\,, \quad \mathrm{c_{grav}} = 23.0\,. \tag{4}$$

SPheno provides the SUSY mass spectrum, and decay branching ratios. With the given parameters the lightest particles turn out to be:

$$m_{\tilde{G}} = 146\,\mathrm{eV}\,, \quad \mathrm{m}_{\tilde{\chi}_1^0} = 151.0\,\mathrm{GeV}\,, \quad \mathrm{m}_{\tilde{\tau}_1^-} = 196.1\,\mathrm{GeV}\,, \quad \mathrm{m}_{\mathrm{h}_0} = 101.5\,\mathrm{GeV}\,. \tag{5}$$

The branching ratio $\sigma(\tilde{\chi}_1^0 \to \tilde{G}\gamma)$ is estimated to be $100\ \%$.

Direct searches at the Large Electron Positron Collider LEP [5–7] and Tevatron [8] did not see any $\tilde{\chi}_1^0 \to \tilde{G}\gamma$ decays, and thus set a lower limit on the neutralino NLSP mass: $m_{\mathrm{NLSP}} > 54\ \mathrm{GeV}$ [7] for neutralinos with any lifetime.

Searches for the lightest neutral Higgs boson in SUSY models, yield in $m_{h_0} > 92.8\ \mathrm{GeV}$ at $95\ \%$ confidence level [9]. Searches for neutralino decays at D0 and CDF, exclude $m_{\tilde{\chi}_1^0} \leq 125\ \mathrm{GeV}$ at $95\ \%$ confidence level [9]. Cosmological constraints on cold gravitino dark matter require $10\ \mathrm{keV} \leq \mathrm{m}_{3/2} \leq 1 - 10\ \mathrm{MeV}$ and a messenger scale $108\ \mathrm{GeV} \leq \mathrm{M_{mess}} \leq 1011\ \mathrm{GeV}$ [10]. Scenarios with smaller gravitino masses and smaller messenger mass scale are cosmologically acceptable, but yield hot gravitino dark matter.

2.2 Event Generation and Simulation

The matrix event generator WHiZard [11–13] is used to generate $100\ \mathrm{fb}^{-1}$ of $e^+e^- \to \tilde{\chi}_1^0\tilde{\chi}_1^0$ reactions at $\sqrt{s} = 500\ \mathrm{GeV}$, as sketched in figure 1. A polarisation of $-80\ \%$ for the e^- and $+60\ \%$ for the e^+ beam, enhances the signal to 217,000 events in $500\ \mathrm{fb}^{-1}$ with respect to 76,000 events without beam polarisation. PYTHIA [14] is used to generate the neutralino decay.

SM background processes are also generated with WHiZard. The following kinematic acceptance cuts are applied [15]:

- 10 GeV jet cut for the minimum invariant mass of a pair of coloured particles
- 4 GeV mass cut for the minimum invariant mass of a pair of colourless particles
- 4 GeV q cut for the minimum $\sqrt{-Q^2}$ for massless t-channel processes.

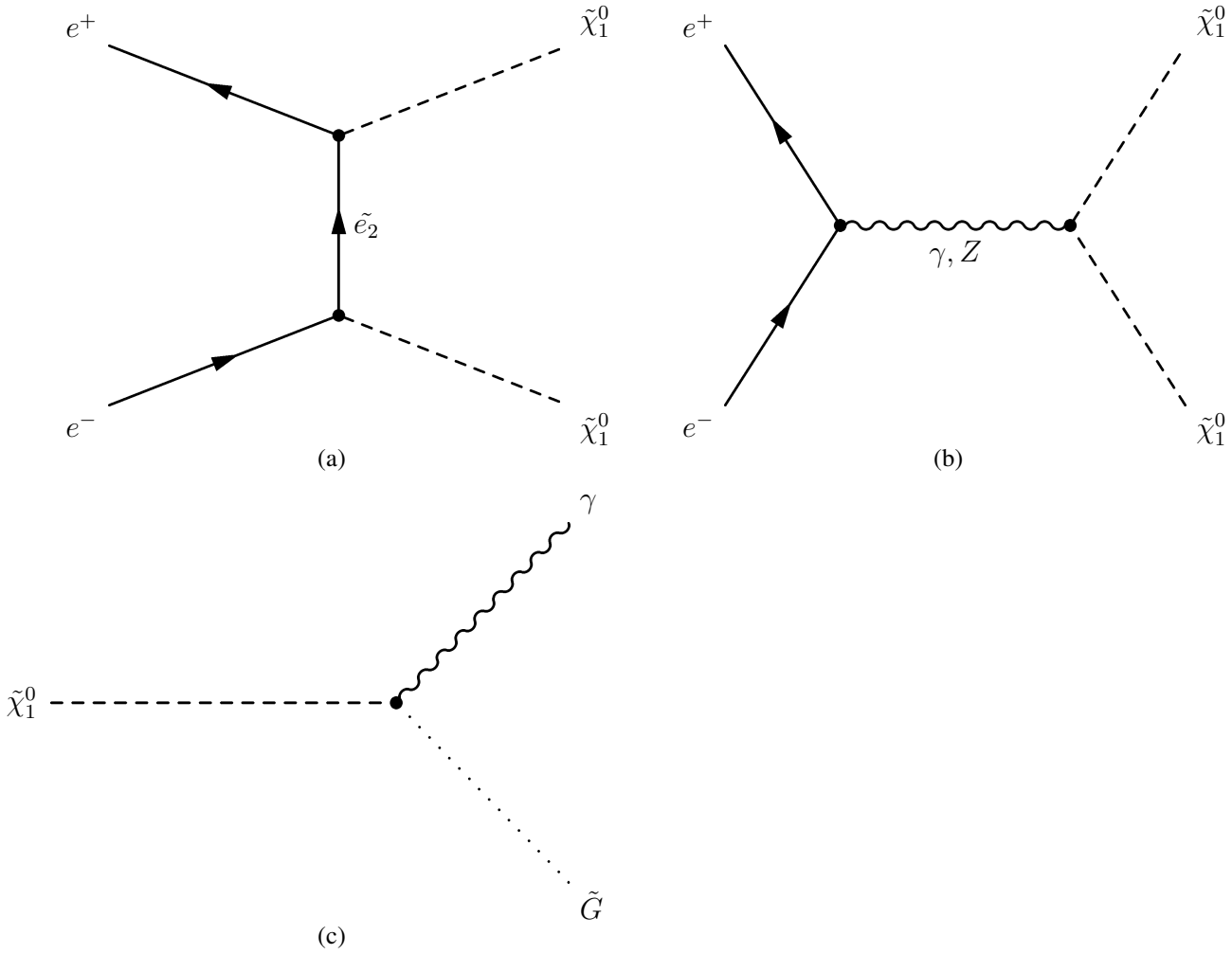

Figure 1: Feynman diagram of $\tilde{\chi}_1^0$ pair production at a lepton collider and $\tilde{\chi}_1^0 \to \tilde{G}\gamma$ decay

SM processes are simulated with a polarisation of $P(e^+, e^-) = (+1, -1)$ and $P(e^+, e^-) = (-1, +1)$. As the required polarisation of $+80$ % for electrons equals 10 % L $+ 90$% R, and accordingly -60 % for positrons equals 80 % L $+ 20$ % R, it can be obtained by mixing 72 % of the $P(e^+, e^-) = (-1, +1)$ with 2 % of the $P(e^+, e^-) = (+1, -1)$ sample. Samples with $P(e^+, e^-) = (-1, -1)$ and $P(e^+, e^-) = (+1, +1)$ polarisation are not available. They correspond to 26 % of the statistics and are not simulated.

For signal and background, the detector simulation is realised with Mokka [16], a detailed simulation based on GEANT4 [17]. The neutralino and gravitino are added to the G4ParticleList, to allow Mokka to track the neutralino through the detector.

The chosen GMSB parameters result in a lifetime of $\tau_{\tilde{\chi}_1^0} = 0.203$ ns. For this study three samples of 0.203 ns, 2.029 ns, and 11.029 ns lifetime, respectively are created with ~ 21000 events each. For a neutralino mass of 151.1 GeV, and energy of 250.0 GeV, this corresponds to a mean decay distance of ~ 11 cm, ~ 80 cm, and ~ 450 cm in the detector, respectively.

Since the s-channel contribution of the signal, as sketched in figure 1, is a process of the weak interaction, it can be enhanced (or suppressed) by polarisation. The left-right asymmetry for an integrated luminosity of 500 fb^{-1} has been calculated on generator level:

$$A_{LR} = \frac{\sigma_{LR} - \sigma_{RL}}{\sigma_{LR} + \sigma_{RL}} = \frac{18.6 \text{ fb} - 433.5 \text{ fb}}{18.6 \text{ fb} + 433.5 \text{ fb}} = -0.92 \tag{6}$$

where σ_{LR} is the signal crossection for an electron beam with -80 % and a positron beam with $+60$ % polarisation, and σ_{RL} is the signal cross section for an electron beam with $+80$ % and a positron beam with -60 % polarisation.

The presented results are obtained for the ILD00 detector model. The electromagnetic calorimeter, which is most important for γ-reconstruction, has an octagonal barrel structure with an inner radius of 185 cm and a z coverage of 235 cm, followed by endcaps with an inner radius of 40 cm and a coverage in z from 245 cm to 264 cm. It is a silicon-tungsten sandwich structure with 19 layers of 0.5 cm, followed by 10 layers of 0.7 cm thickness, corresponding to ≈ 24 X$_0$ integrated depth. The cell size is $0.5 \cdot 0.5$ cm^2, being roughly one third of the Molière radius in tungsten.

The detector geometry and event topology, are displayed in figure 2. Two neutralinos (plotted as green lines) are produced at the IP. They travel into the main tracker, before decaying into a neutral gravitino, and a photon (also displayed as green lines) each. The secondary vertices are clearly visible. The photons shower in the electromagnetic calorimeter (plotted in green), that is surrounded by a hadronic calorimeter (plotted in yellow).

3 Event Reconstruction

The event reconstruction is implemented in the MARLIN [18] framework. The photon reconstruction is realised with a photon-finder-kit [19]. The reconstructed tracks and clusters are then filled into a ROOT [20] tree for further analysis.

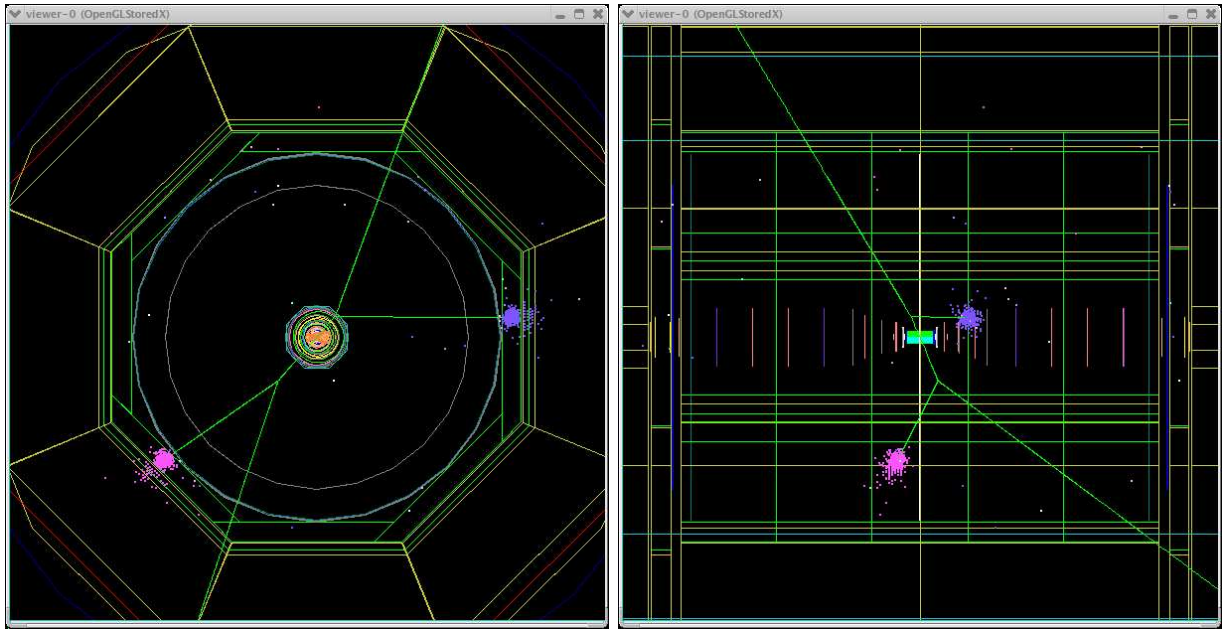

(a) (b)

Figure 2: Event display of an $e^+e^- \to \tilde{\chi}_1^0\tilde{\chi}_1^0$ event in the ILD detector (a) in r - Φ view (b) in Θ - z view

3.1 Photon Reconstruction

The basic principle of the photon reconstruction is sketched in the following, a more detailed description can be found in [19].

Isolated calorimeter hits with less then 4 neighbouring cells being hit, are removed during a topological cleaning step. The remaining ECAL hits are then divided into 10 sub samples, depending on their energy. The chosen thresholds are: 0.1, 1.5, 2.5, 4, 6, 9, 16, 26, 41 and 65 mip per hit. A nearest neighbour clustering algorithm loops over all hits in each sub sample. Only clusters with at least 8 hits are accepted. Depending on the cluster pattern, e.g. their relative position, two clusters are merged to one, or split into two photon seeds. The cosine of the cluster search cone opening angle is chosen to be 0.95, and the distance between two clusters must be larger than 30 mm. In addition fluctuations are suppressed by demanding the ratio of number of hits in one level to those in the previous one to be bigger than 0.4.

Once the clustering is done, the energy of the cluster is estimated from the measured energy, and the threshold-level of the sub sample. This requires proper calibration of the algorithm with single photons at known energy.

Finally, photons are reconstructed. The energy weighted centre of gravity $\vec{\mathrm{cog}}$, is calculated as the sum of hit energy E_i times hit position $\vec{x}_i$ divided by the energy sum of all hits:

$$\vec{\mathrm{cog}} = \frac{\sum_i \vec{x}_i \cdot E_i}{\sum_i E_i} \,. \tag{7}$$

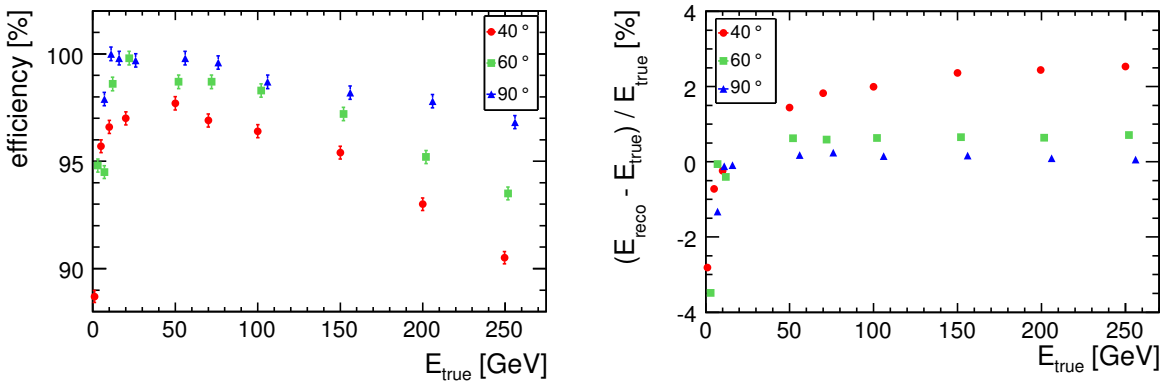

(a) (b)

Figure 3: (a) Single photon efficiency of the photon reconstruction algorithm. (b) Deviation of reconstructed from true photon energy.

The cluster main principle axis is calculated from the energy weighted inertia tensor

$$\mathcal{M} = \sum_i E_i \begin{pmatrix} {dy_i}^2 + {dz_i}^2 & -dx_i dy_i & -dx_i dz_i \\ -dy_i dx_i & {dx_i}^2 + {dz_i}^2 & -dy_i dz_i \\ -dz_i dx_i & -dz_i dy_i & {dx_i}^2 + {dy_i}^2 \end{pmatrix} , \tag{8}$$

where $da = a_{\text{hit}} - a_{\text{cog}}$ for $a \in x, y, z$ is the distance of the hit position to the centre of gravity. The matrix is diagonalised to get the eigenvectors and eigenvalues, which correspond to the inertia axis and momenta. The axis with the smallest momentum is taken as main principle axis and determines the cluster direction.

3.2 Cluster Performance

As shown in figure 3 (a), the efficiency to find exactly one photon, if one photon is shot into the detector is more than $88\ \%$ for 1 to $250\ \text{GeV}$ photons at any incidence angle. As illustrated in figure 3 (b), the deviation between true and reconstructed photon energy, defined as $100 \cdot (E_{\text{reco}} - E_{\text{true}})/E_{\text{true}}$ is smaller then $5\ \%$ for 1 to 250 GeV photons at any incidence angle.

The deviation from reconstructed to true incidence angle is plotted in figure 4. The deviation, in Θ as well as in Φ, is below $1\ \%$ for particles at $90°$ incidence angle and up to $6\ \%$ at $40°$ incidence angle. At energies above $20\ \text{GeV}$, which are relevant for the presented analysis, the deviation between reconstructed and true energy is independent of the particles energy.

The energy resolution for single photons between 1 and $250\ \text{GeV}$ is plotted in figure 5(a). The fit results in:

$$\frac{\sigma_E}{E} = \frac{(16.7 \pm 0.3)\%}{\sqrt{E[\text{GeV}]}} \oplus (0.61 \pm 0.08)\% \, . \tag{9}$$

This is comparable with the energy resolution of $\sigma_E/E = 16.5 \oplus 1.07$, measured with the CALICE Si-W ECAL [21].

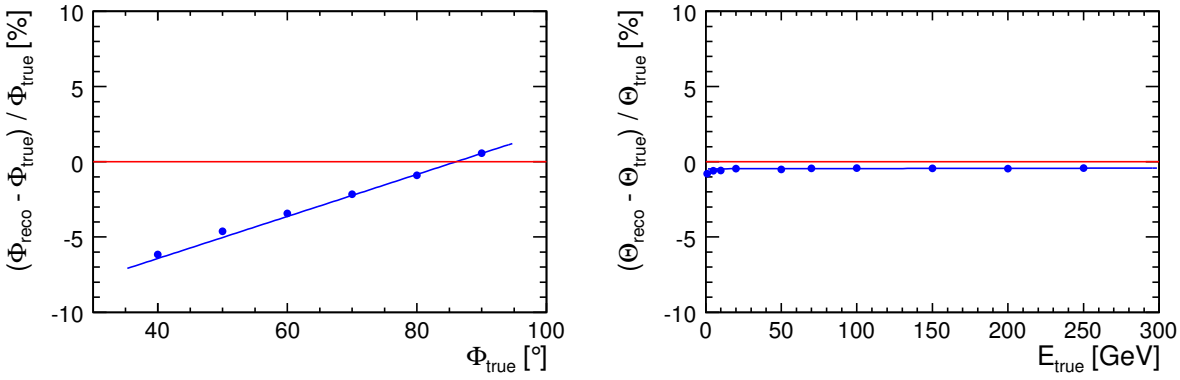

(a) (b)

Figure 4: Deviation of reconstructed from true particle angle in (a) for 100 GeV photons at different Φ angle and (b) for various photon energies in Θ direction.

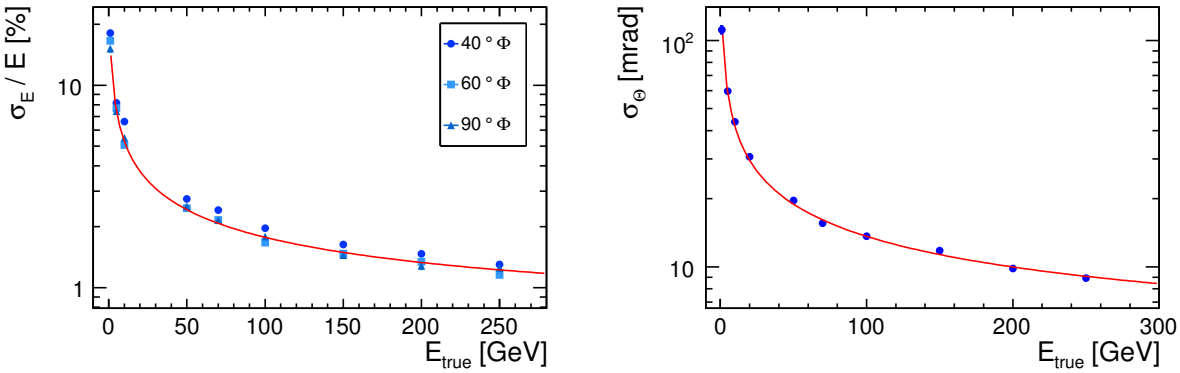

(a) (b)

Figure 5: (a) Energy resolution of the ECAL barrel. (b) Angular resolution of the ECAL barrel.

The angular resolution, plotted in figure 5(b) is determined to be

$$\sigma_\theta = \frac{(131 \pm 2)\ \text{mrad}}{\sqrt{E\ [\text{GeV}]}} \oplus (3.7 \pm 0.5)\ \text{mrad}. \tag{10}$$

4 Signal Selection

At the ILC 500 fb^{-1} integrated luminosity at $\sqrt{s} = 500$ GeV with $+80$ % electron and -60 % positron polarisation, correspond to 216,728 signal events. In addition, there will be

$$2,001,046\ \nu_e\overline{\nu_e}\gamma\gamma\ , \quad 70,319\ \nu_\mu\overline{\nu_\mu}\gamma\gamma\ , \quad 70,674\ \nu_\tau\overline{\nu_\tau}\gamma\gamma\ , \quad 3,113,697\ \gamma\gamma \tag{11}$$

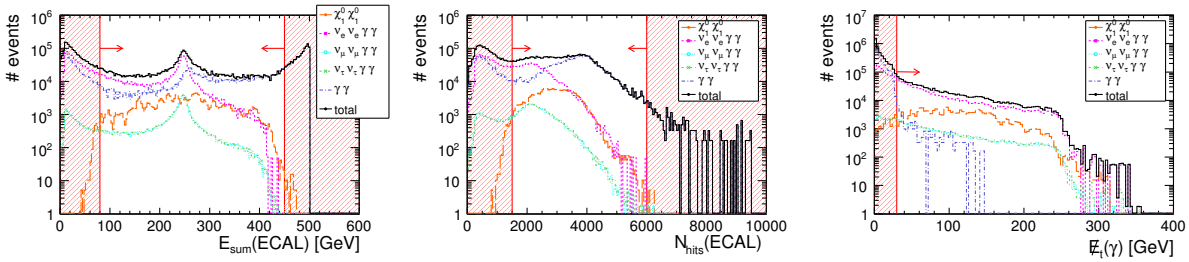

(a) (b) (c)

Figure 6: (a)Energy sum and (b) number of hits distributions in the ECAL, as well as (c) missing transverse energy per event for signal (orange dots) and background without any selection cuts applied.

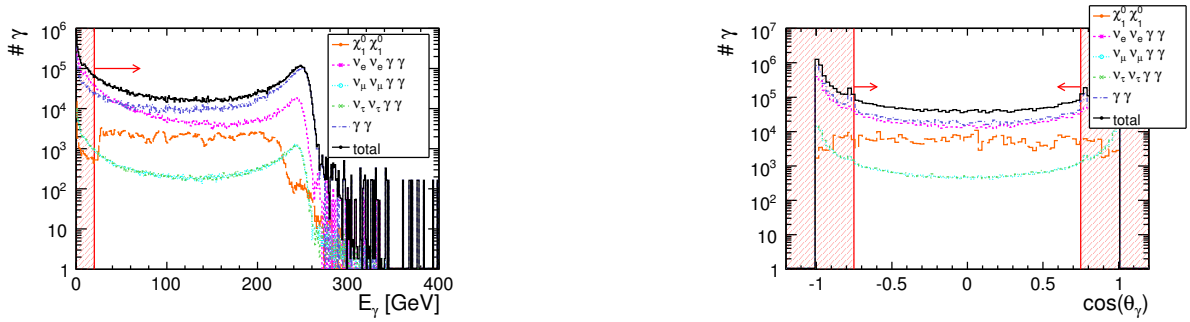

(a) (b)

Figure 7: (a) Photon energy and (b) $\cos\Theta$ distribution for signal (orange dots) and background without any selection cuts applied.

events.

Those are summing up to 5.3 million background events, corresponding to a signal to background ratio of $\mathrm{S} : \mathrm{B} \approx 1 : 24.3$.

To separate signal from background events, the signature in the electromagnetic calorimeter (ECAL) is utilised. Figure 6 and figure 7 show the relevant distributions before all cuts for signal process (orange dots), background processes and combined signal (black line). The vertical red lines indicate the chosen cuts. The signatures left in other sub detectors, e.g. the BeamCal and the HCAL, are not taken into account for this analysis.

The applied selection cuts are:

- number of hits in ECAL $1500 < \#\mathrm{hits} < 6000$
- energy sum in ECAL $80\ \mathrm{GeV} < \mathrm{E_{sum}} < 450\ \mathrm{GeV}$
- missing transverse energy $\not{E}_\mathrm{t} > 20\ \mathrm{GeV}$

	$E_{\text{sum}}(ECAL)$	$N_{\text{hits}}(ECAL)$	$\not{E}_{\text{t}}$	at least two γ with $E_\gamma > 20$ GeV	at least two γ with $\lvert\cos(\theta_\gamma)\rvert < 0.75$	all cuts
$\tilde{\chi}_{\tau:0.2\text{ns}}$	99.1 %	98.7 %	92.3 %	99.1 %	65.7 %	59.5 %
$\tilde{\chi}_{\tau:2.0\text{ns}}$	95.7 %	93.0 %	91.1 %	89.0 %	60.2 %	53.7 %
$\tilde{\chi}_{\tau:11.0\text{ns}}$	52.5 %	40.3 %	60.3 %	18.9 %	13.9 %	10.2 %
$\nu_e\nu_e\gamma\gamma$	53.4 %	45.2 %	46.6 %	20.1 %	6.8 %	1.4 %
$\nu_\mu\nu_\mu\gamma\gamma$	78.2 %	66.8 %	69.4 %	28.4 %	6.4 %	2.3 %
$\nu_\tau\nu_\tau\gamma\gamma$	78.6 %	71.2 %	67.3 %	28.2 %	6.5 %	2.3 %
$\gamma\gamma$	40.6 %	69.9 %	1.0 %	28.3 %	9.3 %	0.04 %

Table 1: Relative amount of events surviving each single cut.

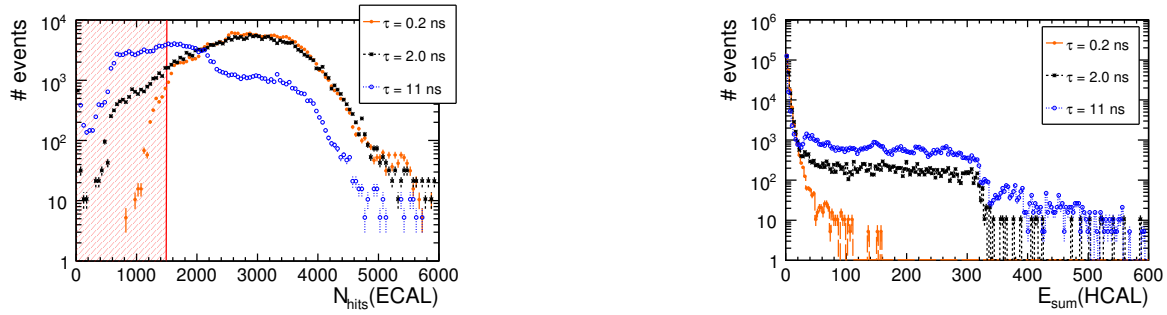

(a) (b)

Figure 8: Long-lived neutralinos may decay late in the ECAL, resulting in a shower leaking to the HCAL: (a) number of hits per event in the ECAL for two neutralino lifetimes (b) energy sum per event in the HCAL for two neutralino lifetimes

- at least two photons with

  energy $E_\gamma > 20$ GeV

  $\lvert\cos(\theta_\gamma)\rvert < 0.75$

Requiring all the above criteria reduces the background to 0.6 % of the original amount, while leaving 59.5 % of the $\tilde{\chi}_1^0$ with $\tau = 0.2$ ns corresponding to a $\text{S} : \text{B} \approx 3.9 : 1$, 53.7 % of the $\tau = 2.0$ ns sample corresponding to a $\text{S} : \text{B} \approx 3.5 : 1$, and 10.2 % of the $\tau = 11.0$ ns signal sample, corresponding to a $\text{S} : \text{B} \approx 1 : 1.5$ respectively. Table 1 gives a more detailed overview on the effect of each single cut on the different types of background and signal. Quoted is the percent of surviving events applying one cut at a time, and all cuts at once.

Figure 8 illustrates that longer-lived neutralinos only decay late within the electromagnetic calorimeter. This results in energy-leakage to the hadronic calorimeter, which is not included in the photon reconstruction. Thus, samples with longer lifetimes are more sensitive to cuts on the required ECAL energy and number of hits.

5 Results

For an integrated luminosity of $\mathcal{L} = 500\ \mathrm{fb}^{-1}$ at $500\ \mathrm{GeV}$ centre of mass energy with $+80\ \%$ polarised electron and $-60\ \%$ polarised positron beam, the measured signal cross section is defined as:

$$\sigma = \frac{N_{\mathrm{signal}}}{\epsilon \cdot \mathcal{L}} \tag{12}$$

for $N_{\mathrm{signal}} = N_{\mathrm{generated}} \cdot \epsilon$ selected signal events. Given the selection efficiency ϵ as stated in table 1, this results in

- $\sigma = 433.5 \pm 1.1$ fb for $\tau_{\mathrm{true}} = 0.2$ ns
- $\sigma = 433.5 \pm 1.2$ fb for $\tau_{\mathrm{true}} = 2.0$ ns
- $\sigma = 433.4 \pm 3.9$ fb for $\tau_{\mathrm{true}} = 11.0$ ns

5.1 $\tilde{\chi}_1^0$ mass

Since the process $e^+e^- \rightarrow \tilde{\chi}_1^0\tilde{\chi}_1^0$ is the only SUSY process allowed by kinematics, the lower and upper edge of the photon energy distribution is given by [22]

$$E^{\gamma}_{\mathrm{min,max}} = \frac{1}{4}\left(\sqrt{s} \mp \sqrt{s - 4m^2_{\tilde{\chi}_1^0}}\right) . \tag{13}$$

And thus, the neutralino mass is

$$m_{\tilde{\chi}_1^0} = \frac{1}{2}\sqrt{s \mp \left(4 \cdot E^{\gamma}_{\mathrm{min,max}} - \sqrt{s}\right)^2} , \tag{14}$$

where $\sqrt{s} = 500\ \mathrm{GeV}$ is the centre of mass energy. The lower edge can be washed out by, e.g. SM background processes with soft photons, whereas the upper edge is always resulting from decays of directly pair-produced neutralinos.

Figure 9 displays the reconstructed photon energy in the upper row, while the energy distribution from MonteCarlo is shown in the lower row. The left column represents the pure signal distribution without any selection cuts, and the right column contains signal and background after all selection cuts. As indicated by the red line, the upper edge is fitted with:

$$E_{\gamma}(A, m^2_{\tilde{\chi}_1^0}, S, B) = A/\left(1 + \exp\left[\frac{E + \frac{1}{4}\left(\sqrt{s} + \sqrt{s - 4m^2_{\tilde{\chi}_1^0}}\right)}{S}\right]\right) + B . \tag{15}$$

The amplitude A, slope S, background B and neutralino mass $m_{\tilde{\chi}_1^0}$ are free fitting parameters. The fit is performed in ROOT [20]. For the $\tau_{\chi} = 2.0$ ns signal sample including the full background, and a true neutralino mass of $m_{\tilde{\chi}_1^0} = 151.0\ \mathrm{GeV}$, the mass obtained for the reconstructed photon energy m_{reco}, and the photon energy from MonteCarlo truth information m_{MC} after all selection cuts, are listed in table 2

The fact that the reconstructed photon energy tends to give smaller values then the real neutralino mass, while the spectrum using MonteCarlo truth information rather overestimates the neutralino mass can be corrected by calibrating both, MonteCarlo and reconstructed mass with the true mass, for different neutralino masses.

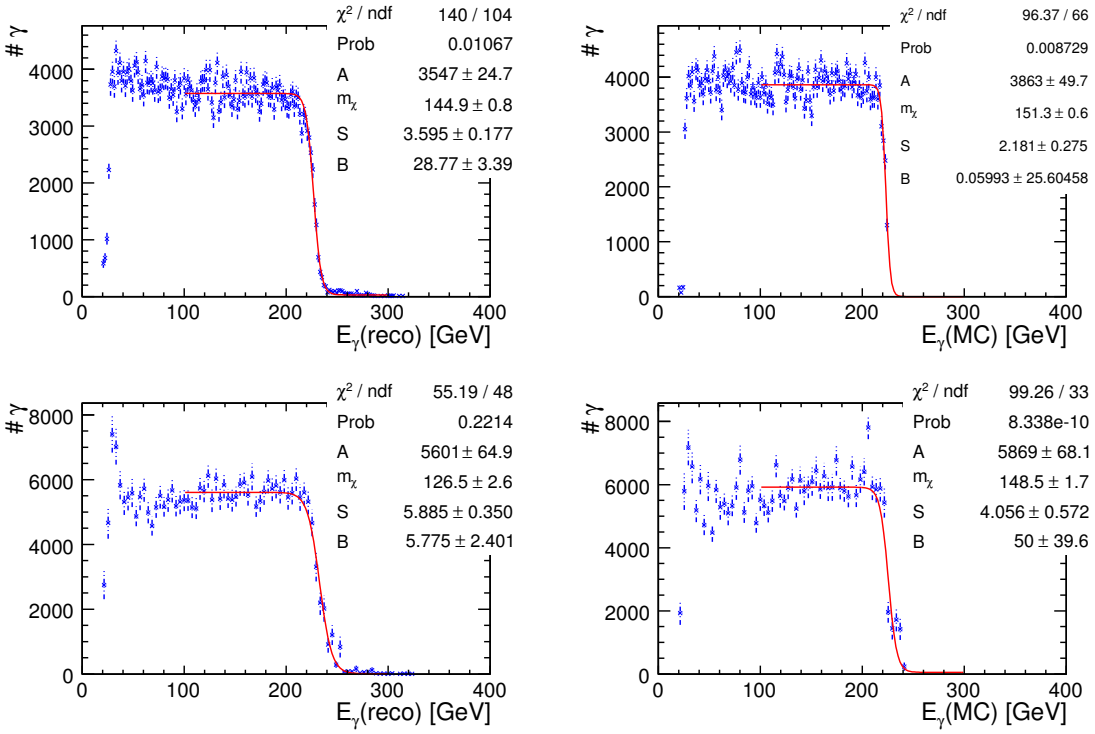

Figure 9: Mass determination from photon energy distribution from neutralinos with 2.0 ns lifetime after reconstruction (upper row) and from MonteCarlo information (lower row). Plots in the left column show signal only, without selection cuts. Plots in the right columns include signal plus background after all selection cuts.

	signal only no cuts	signal plus background after cuts
$m_{\rm reco}$	144.9 ± 0.8 GeV	126.5 ± 2.6 GeV
$m_{\rm MC}$	154.9 ± 0.5 GeV	148.5 ± 1.7 GeV

Table 2: Neutralino mass as reconstructed from the photon energy distribution.

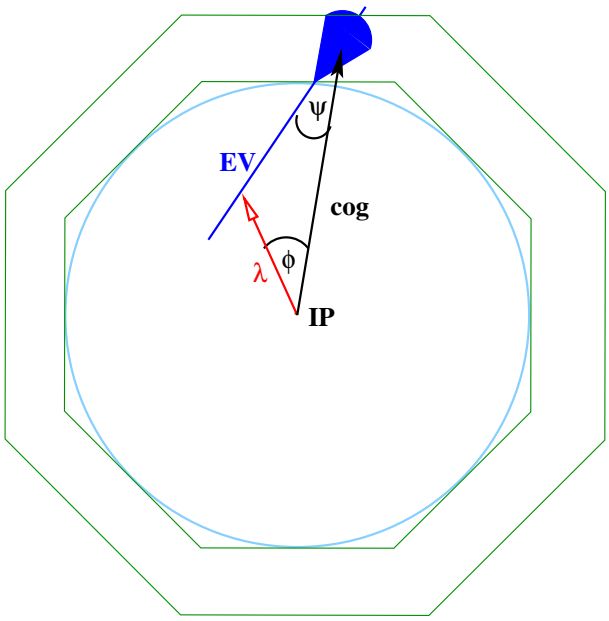

Figure 10: Reconstruction principle of the neutralino flight distance (λ). The photon shower centre of gravity (cog), main axis of inertia (EV), and the angle in between (ψ) can be measured. The angle between photon and neutralino (ϕ) is given by kinematic constraints.

5.2 $\tilde{\chi}_1^0$ lifetime

The spatial energy distribution of a photon in the highly granular ECAL allows to determine the energy weighted centre of gravity $\vec{\text{cog}}$, and the principal axis of inertia $\vec{\text{EV}}$, which define the direction of the incoming photon, indicated in figure 10. As described in [22], it is possible to determine the neutralino decay angle ϕ from the measured photon energy E_γ:

$$\cos\phi = \frac{E_0}{p_0} - \frac{m^2_{\tilde{\chi}_1^0}}{2 \cdot p_0 E_\gamma} \,, \tag{16}$$

where E_0 is the nominal beam energy and $p_0 = \sqrt{E_0 - m_{\tilde{\chi}_1^0}}$ corresponds to the neutralino momentum. The explicit occurrence of the neutralino mass, emphasises the importance of an accurate measurement, as described above. The neutralino flight distance can be calculated according to

$$\lambda = |\vec{\text{cog}}| \cdot \frac{\sin\psi}{\sin\phi}. \tag{17}$$

Here ψ is the angle between the photon-shower centre of gravity $\vec{\text{cog}}$ and the principal axis of inertia $\vec{\text{EV}}$.

The pure neutralino decay spectra shown in figure 11 follow an exponential distribution convoluted with the Gaussian shaped detector resolution that can be described with a decay model, as it is implemented in RooFit [23]. It is convoluted with the Standard Model background displayed in the upper left plot in figure 12. The lifetime distribution is fitted with:

$$f(t) = f_{\text{sig}} \cdot \left(\exp\left[\frac{-t}{\tau}\right] \otimes \frac{1}{\sigma\sqrt{2\pi}} \exp\left[-\frac{t'^2}{2}\right] \right) \otimes f_{\text{bkg}} \left(\frac{1}{\sigma\sqrt{2\pi}} \exp\left[-\frac{t'^2}{2}\right] \right) \,, \tag{18}$$

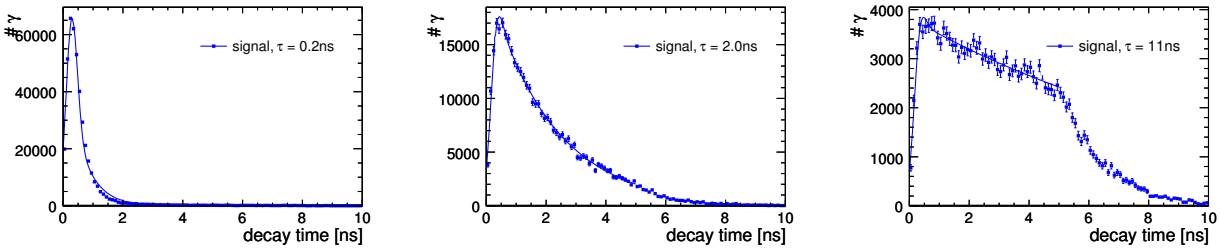

(a) (b) (c)

Figure 11: Neutralino lifetime reconstruction using MC_{truth} information (a) 0.2 ns (b) 2.0 ns and (c) 11.0 ns input lifetime, respectively. Plotted is only the signal without any selection cuts applied.

	$\tau_{\text{reco}}[\text{ns}]$		
	$\tau_{\text{true}} = 0.2\text{ns}$	$\tau_{\text{true}} = 2.0\text{ns}$	$\tau_{\text{true}} = 11.0\text{ns}$
no cut	0.575 ± 0.002	2.13 ± 0.01	10.9 ± 0.3
E_{sum}	0.575 ± 0.002	2.13 ± 0.01	10.5 ± 0.3
#hits	0.573 ± 0.002	2.14 ± 0.01	11.2 ± 0.3
$\not{E}_{\text{t}}$	0.569 ± 0.002	2.10 ± 0.01	10.3 ± 0.2
at least two γ with			
E_γ	0.577 ± 0.002	2.14 ± 0.01	11.1 ± 0.4
$\lvert\cos(\theta_\gamma)\rvert$	0.498 ± 0.002	2.20 ± 0.01	15.0 ± 0.9
all cuts	0.477 ± 0.002	2.8 ± 0.01	10.9 ± 0.5

Table 3: Influence of the selection cuts on the neutralino lifetime reconstruction for the signal only samples.

where f_{sig} and f_{bkg} represent the fraction of signal and background events, respectively. The Gaussian parameter

$$t' = \frac{t - \mu}{\sigma} \tag{19}$$

includes the width σ, that expresses the experimental resolution on each measurement of the lifetime t. The mean value μ parametrises the average bias on that measurement. The underlying Gaussian is assumed to be a result of the detector resolution, and therefore is taken to be the same for signal and background. The mean and width are determined from the fit to the background only sample, and are subsequently fixed for the data sample.

The cut parameters applied to reduce the number of background events, may not influence the lifetime measurement. The result of each single cut, and the combination of all cuts, on the reconstructed neutralino lifetime τ_{reco} of the signal only sample, are listed in table 3, including statistical errors.

The data samples include signal and background after all selection cuts. Assuming the Standard Model background is known with very high precision, the fit resulting from the background only sample is subtracted from the data sample. The resulting lifetime distribution, plotted in figure 12, is fitted from 0 to 5 ns with equation 5.2.

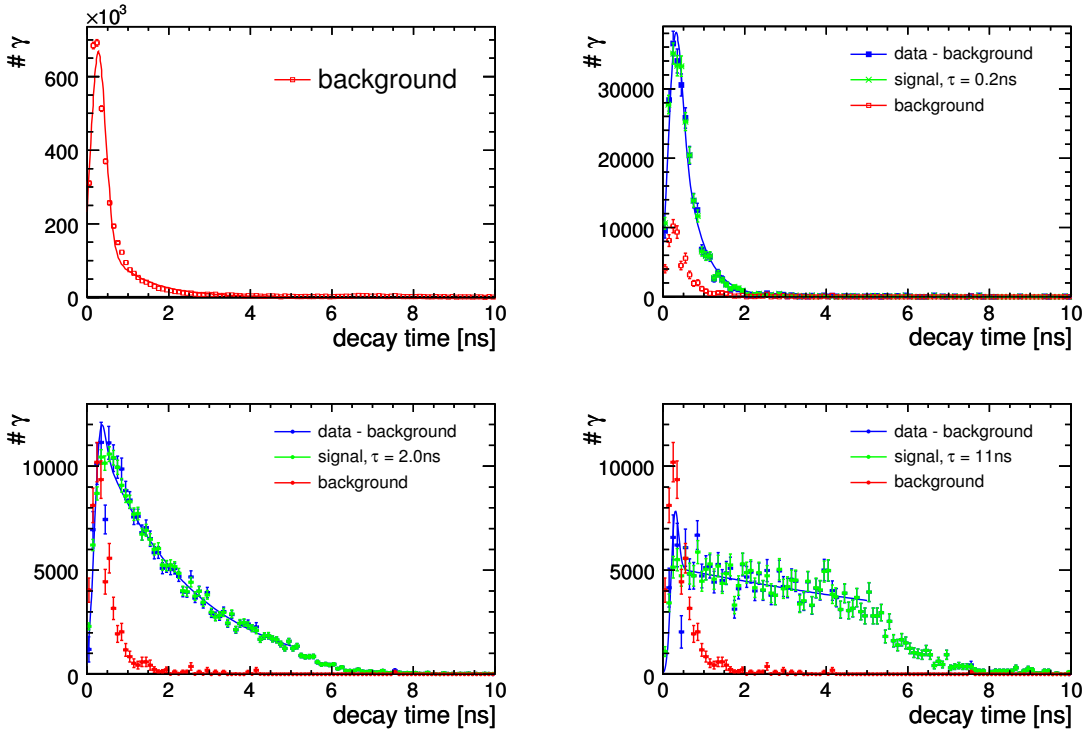

Figure 12: Neutralino lifetime reconstruction from the kinematic method for SM background reconstruction (upper left) neutralinos with 0.2 ns (upper right) 2.0 ns (lower left) and 11.0 ns (lower right) input lifetime, respectively. Plotted is signal only (green open dots) and background subtracted data (blue squares) after all selection cuts

	$\tau_{\text{true}} = 0.2$ ns	$\tau_{\text{true}} = 2.0$ ns	$\tau_{\text{true}} = 11.0$ ns
f_{sig} [%]	60.7 ± 0.2	94.4 ± 0.1	97.1 ± 0.1
μ [ns]	$0.27 \pm \text{const}$	$0.27 \pm \text{const}$	$0.27 \pm \text{const}$
σ [ns]	$0.19 \pm \text{const}$	$0.19 \pm \text{const}$	$0.19 \pm \text{const}$
τ_{reco} [ns]	0.471 ± 0.002	2.182 ± 0.010	11.39 ± 0.56

Table 4: Neutralino lifetime fit results for the signal + background samples of different input lifetimes.

The obtained fitting results and lifetimes with their corresponding statistical errors for the signal plus background samples after all selection cuts, subtracted by the background fit, are listed in table 4.

The reconstructed lifetime of the $\tau_{\text{true}} = 2.0$ ns neutralino sample is well in agreement with the input values.

For the earlier decaying $\tau_{\text{true}} = 0.2$ ns sample, the reconstructed lifetime is longer then the input lifetime. Due to the limited detector resolution and the applied reconstruction algorithm, the background sample is also reconstructed with a lifetime of a few hundred picoseconds.

In principle the lifetime distribution is expected to be peaked at 0 ns. Following an exponential distribution, most neutralinos are expected to decay immediately. Even if the limited detector resolution is taken into account, the lifetime distribution is broadened by an underlying Gaussian distribution, but should still be centred around 0 ns. As shown in figure 4, with the current detector configuration and reconstruction algorithm the angular reconstruction is systematically below the true shower angle. At 40° incidence angle, the reconstructed angle is $6.15\,\%$ off. This is shifting the mean value. It can be improved by fine tuning the reconstruction algorithm.

The signal lifetime determination could be improved by taking advantage from photons undergoing pair production in the TPC, which occurs in $15\,\%$ of the events.

The long lifetime scenario on the other hand is challenging due to the limited detector size. With an average lifetime of 11 ns many neutralinos decay late in the ECAL or even behind and cause leakage. The applied selection cuts, withdraw neutralinos that do not decay within the ECAL. They could be recovered by extending the clustering algorithm towards the HCAL. This scenario would also profit from the usage of timing information, which is not available in the current simulation.

References

[1] S. P. Martin, "A supersymmetry primer," arXiv:hep-ph/9709356.

[2] J. L. Feng and M. M. Nojiri, "Supersymmetry and the linear collider," arXiv:hep-ph/0210390.

[3] W. Porod, "SPheno, a program for calculating supersymmetric spectra, SUSY particle decays and SUSY particle production at e+ e- colliders," *Comput. Phys. Commun.* **153** (2003) 275–315, arXiv:hep-ph/0301101.

[4] M. Battaglia *et al.*, "Physics benchmarks for the ilc detectors," arXiv:hep-ex/0603010.

[5] K. Klein, "Searches for gauge mediated SUSY breaking at LEP," arXiv:hep-ex/0205096.

[6] **OPAL** Collaboration, G. Abbiendi *et al.*, "Searches for gauge-mediated supersymmetry breaking topologies in e+ e- collisions at LEP2," *Eur. Phys. J.* **C46** (2006) 307–341, arXiv:hep-ex/0507048.

[7] **ALEPH** Collaboration, A. Heister *et al.*, "Search for gauge mediated SUSY breaking topologies in e+ e- collisions at centre-of-mass energies up to 209-GeV," *Eur. Phys. J.* **C25** (2002) 339–351, arXiv:hep-ex/0203024.

[8] **SUSY Working Group** Collaboration, R. L. Culbertson *et al.*, "Low-scale and gauge-mediated supersymmetry breaking at the Fermilab Tevatron Run II," arXiv:hep-ph/0008070.

[9] **Particle Data Group** Collaboration, C. Amsler *et al.*, "Review of particle physics," *Phys. Lett.* **B667** (2008) 1.

[10] G. Moultaka, "Very Light Gravitino Dark Matter," *Acta Phys. Polon.* **B38** (2007) 645–652, arXiv:hep-ph/0612331.

[11] W. Kilian, T. Ohl, and J. Reuter, "WHIZARD: Simulating Multi-Particle Processes at LHC and ILC," arXiv:0708.4233 [hep-ph].

[12] W. Kilian, "WHIZARD 1.0: A generic Monte-Carlo integration and event generation package for multi-particle processes. Manual,". LC-TOOL-2001-039.

[13] M. Moretti, T. Ohl, and J. Reuter, "O'Mega: An optimizing matrix element generator," arXiv:hep-ph/0102195.

[14] T. Sjostrand, S. Mrenna, and P. Skands, "PYTHIA 6.4 physics and manual," *JHEP* **05** (2006) 026, arXiv:hep-ph/0603175.

[15] "Standard Model Data Samples web site." http://confluence.slac.stanford.edu/display/ilc/Standard+Model+Data+Samples.

[16] P. Mora de Freitas and H. Videau, "Detector Simulation with Mokka and Geant4: Present and Future," Tech. Rep. LC-TOOL-2003-010, LC Note, mar, 2003. http://mokka.in2p3.fr.

[17] The Geant4 Collaboration, S. Agostinelli, *et al.*, "Geant4: A simulation toolkit," *Nucl. Instrum. Meth.* **A506** (2003) 250–303.

[18] F. Gaede, "Marlin and LCCD: Software tools for the ILC," *Nucl. Instrum. Meth.* **A559** (2006) 177–180.

[19] P. Krstonosic, "Measurement of Quartic Boson Couplings at the International Linear Collider and Study of Novel Particle Flow Algorithms,". DESY-THESIS-2008-007.

[20] R. Brun and F. Rademakers, "ROOT: An object oriented data analysis framework," *Nucl. Instrum. Meth.* **A389** (1997) 81–86.

[21] **CALICE** Collaboration, C. Adloff *et al.*, "Response of the CALICE Si-W Electromagnetic Calorimeter Physics Prototype to Electrons," *J. Phys. Conf. Ser.* **160** (2009) 012065, arXiv:0811.2354 [physics.ins-det].

[22] S. Ambrosanio and G. A. Blair, "Measuring gauge-mediated supersymmetry breaking parameters at a 500-gev e+ e- linear collider," *Eur. Phys. J.* **C12** (2000) 287–321, arXiv:hep-ph/9905403.

[23] W. Verkerke and D. Kirkby, "The RooFit toolkit for data modeling," arXiv:physics/0306116.